Remarks

Claims 1-23, 27 and 28 were pending in the subject application. By this Amendment, the applicants have amended claims 1, 3 and 6, have added new dependent claims 29 and 30, and have cancelled claims 10 and 11; entry of the amendments is respectfully requested. The applicants acknowledge that claims 20-23, 27 and 28 have been withdrawn as being directed to non-elected subject matter. The applicants respectfully submit that no new matter has been added by these amendments. Accordingly, claims 1-23, 27 and 28-30 are now before the Examiner for consideration.

The amendments to the claims have been made in an effort to lend greater clarity to the claimed subject matter and to expedite prosecution. Support for the claim amendments and new claims can be found throughout the specification. The amendments should not be taken to indicate the applicants' agreement with, or acquiescence to, any of the rejection(s) of record. Favorable consideration of the claims now presented, in view of the remarks and amendments set forth herein, is earnestly solicited.

As an initial matter, the Examiner has objected to the subject specification due to informalities. Specifically, the Examiner indicates that the subject specification did not include sequence identifiers for sequences disclosed in Figure 4. By this Amendment, the applicants have attached a replacement Figure 4a and 4b (pages 4/13, 5/13 and 6/13 of the figures) to include sequence identifiers for the sequences. Applicants have also amended the description of Figure 4a and 4b in the specification to include sequence identifiers.

Claims 1-16 and 19 have been rejected under 35 U.S.C. §112, first paragraph, on the grounds that the subject specification does not provide adequate written description. The Examiner asserts that "the instant case specification fails to disclose representative number of species by structure and function encompassed by the genus as claimed i.e. recombinant genetic material for the production of hetrodimeric specific wild-type or chimeric TCR with any antigen specificity, wherein any and all domains (i.e. extracellular, transmembrane and intracellular domains) of the TCR-complex has been modified by random mutagenesis." The applicants respectfully traverse this ground of rejection and assert that there is adequate written description for the claimed invention. The applicants note that

the claimed method encompasses "rational mutagenesis" and not "random mutagenesis" as has been suggested by the Examiner in the Office Action. In addition, the applicants note that particular amino acids are described in the specification that are now recited in claim 1. Thus, it is to be noted that amended claim 1 recites that the externally provided TCR-chains do pair but do not form mixed pairs with the endogenous chains of the T-cells; that there is no impairment of the functionality and stability of the heterodimeric TCR; that there is a rational mutagenesis of amino acid-surfaces as compared with the initial amino acid-surface(s); and that specific amino acid changes are indicated. The applicants respectfully assert that a sufficient number of species are described in the specification to support the genus of the claimed invention. The applicants respectfully assert that a person of ordinary skill in the art, having considered the teachings of the subject specification, would understand that the applicants were in possession of the claimed invention. Accordingly, reconsideration and withdrawal of the rejection under 35 U.S.C. §112, first paragraph, is respectfully requested.

Claims 1-19 have been rejected under 35 U.S.C. §112, first paragraph, as nonenabled by the subject specification. The applicants respectfully assert that the subject specification enables the claimed invention.

Under this rejection, the Examiner asserts that "an understanding the structure and mechanics of activating immune receptors is crucial for the development of accurate models of any TCR functionality..." (page 7, bottom paragraph, of the Office Action) (emphasis added). In contrast to what is stated in the Office Action, the present invention relates to a method for producing specific modified recombinant TCR-chains and TCRs. Indeed, TCR receptors of the claimed method have to maintain their functionality and stability. The subject application provides a person of ordinary skill in the art with *all* essential information for practicing the claimed invention, including a) how to make mutated TCRs, b) how to introduce them into cells, and c) how to test these TCR for functionality. Using this information, the person of ordinary skill in the art is enabled to practice the invention as claimed.

The applicants again note that mutations as introduced in the first or second TCR chains are not "random" mutations as has been suggested by the Examiner, but rather are based on a rational

design that has been developed using empirical protein-crystal structures. Both the human and murine structures are very similar due to their "immunglobulin-like folds" in the ecto-domains, and thus this allow(s) for inter-species design. The applicants have also attached a publication by Voss *et al.* (2007) that shows that the claimed method can be used in order to modify a human TCR having specificity for gp100. Thus, it was clear at the time of filing of the subject application that the claimed method could be used for numerous species, including both for murine and human TCRs.

It should be noted that the requirement for some experimentation and/or screening does not necessarily render a claim non-enabled. "Enablement is not precluded by the necessity for some experimentation such as routine screening. . . A considerable amount of experimentation is permissible, if it is merely routine . . ." (emphasis added). *In re Wands*, 8 USPQ 2d 1400, 1404 (Fed. Cir. 1988). In the case of the subject application, any experimentation needed would be routine given the guidance provided in the subject application.

For the reasons set forth above, the applicants believe that they have fulfilled the requirements of 35 U.S.C. §112. Accordingly, reconsideration and withdrawal of the rejection under 35 U.S.C. §112, first paragraph, is respectfully requested.

In view of the foregoing remarks and amendments to the claims, the applicants believe that the currently pending claims are in condition for allowance, and such action is respectfully requested.

The Commissioner is hereby authorized to charge any fees under 37 CFR §§1.16 or 1.17 as required by this paper to Deposit Account No. 19-0065.

The applicants also invite the Examiner to call the undersigned if clarification is needed on any of this response, or if the Examiner believes a telephone interview would expedite the prosecution of the subject application to completion.

Respectfully submitted,

Doran R. Pace
Patent Attorney
Registration No. 38,261
Phone: 352-375-8100
Fax No.: 352-372-5800
Address: P.O. Box 142950
Gainesville, FL 32614-2950

DRP/la

Attachments: Replacement Figures 4a-4b
Copy of Voss *et al.* (2007)

Molecular Design of the C$\alpha\beta$ Interface Favors Specific Pairing of Introduced TCR$\alpha\beta$ in Human T Cells[1]

Ralf-Holger Voss,[2]* Ralph A. Willemsen,[†] Jürgen Kuball,[‡] Margarete Grabowski,* Renate Engel,[§] Ratna S. Intan,* Philippe Guillaume,[¶] Pedro Romero,[‖] Christoph Huber,* and Matthias Theobald[‡]

A promising approach to adoptive transfer therapy of tumors is to reprogram autologous T lymphocytes by TCR gene transfer of defined Ag specificity. An obstacle, however, is the undesired pairing of introduced TCRα- and TCRβ-chains with the endogenous TCR chains. These events vary depending on the individual endogenous TCR and they not only may reduce the levels of cell surface-introduced TCR but also may generate hybrid TCR with unknown Ag specificities. We show that such hybrid heterodimers can be generated even by the pairing of human and mouse TCRα- and TCRβ-chains. To overcome this hurdle, we have identified a pair of amino acid residues in the crystal structure of a TCR that lie at the interface of associated TCR Cα and Cβ domains and are related to each other by both a complementary steric interaction analogous to a "knob-into-hole" configuration and the electrostatic environment. We mutated the two residues so as to invert the sense of this interaction analogous to a charged "hole-into-knob" configuration. We show that this inversion in the CαCβ interface promotes selective assembly of the introduced TCR while preserving its specificity and avidity for Ag ligand. Noteworthily, this TCR modification was equally efficient on both a Mu and a Hu TCR. Our data suggest that this approach is generally applicable to TCR independently of their Ag specificity and affinity, subset distribution, and species of origin. Thus, this strategy may optimize TCR gene transfer to efficiently and safely reprogram random T cells into tumor-reactive T cells. *The Journal of Immunology*, 2008, 180: 391–401.

One of the aims of cellular immune therapy for human (Hu)[3] malignancies is the identification and propagation of autologous tumor-associated Ag (TAA)-specific T lymphocytes. To circumvent the cumbersome generation of tumor-specific T cells, the genetic transfer of tumor Ag-specific TCR has been proposed as alternative strategy to redirect the immune system against cancer cells. This strategy is currently being pursued in its first clinical trials (1).

Central tolerance mechanisms in the thymus eliminate high-affinity TCR for self-Ag and thus diminish the frequency of potent tumor-reactive CTL in the Hu T cell repertoire (2). To bypass this restriction, we took advantage of HLA-A2-transgenic (Tg) mice to develop in vivo murine (Mu) high-affinity TCR (3, 4). Alternative strategies focus on in vitro techniques such as phage (5)/yeast (6)/TCR (7) display. The retroviral transfer of the related TCR genes into T cells preserved both effector efficacy and memory pool formation in vivo (8).

Upon transduction of T cells with TCR, mixed pairing of introduced and endogenous TCRα- and TCRβ-chains may generate a plethora of hybrid TCR of unknown specificities and potential autoimmune reactivities (9). In this regard, the size of the T cell repertoire is theoretically highly diverse in the order of 10^{15}. However, it contracts several orders of magnitude depending on thymic output, aging, and homeostasis of the individual (10). Additionally, introduced TCR may have to compete with endogenous TCR for assembly into the CD3 complex and subsequent cell surface export (11).

To prevent the formation of hybrid TCR, three-domain single chain TCR were generated whose variable domains were covalently attached to each other by a linker. Effector function was improved by fusion to signaling molecules such as CD3ζ or Lck (12, 13). Additionally, chimerization of double chain TCR to CD3ζ resulted in preferential heterodimerization due to the transmembrane dimerization motif located in CD3ζ (13). Recently, the introduction of an artificial disulfide bond in the constant domains yielded stable TCR suited for both phage display (5) and gene therapy (14, 15). "Murinization" of Hu domains led to preferential pairing (16, 17). However, concerns associated with such chimeric TCR are their immunogenicity, interference with appropriate signaling, and residual pairing with endogenous TCR.

Analysis of the crystal structures of the alloreactive H-2K^b-restricted Mu 2C TCR (18) and a Hu HLA-A*0201-restricted TCR

*Medical Clinic (III) and Polyclinic, Department of Hematology and Oncology, Johannes Gutenberg-University, Mainz, Germany; [†]Laboratory of Tumor Immunology, Department of Medical Oncology, Erasmus Medical Center Daniel den Hoed Cancer Center, Rotterdam, The Netherlands; [‡]Department of Hematology and Van Creveld Clinic, University Medical Center, Utrecht, The Netherlands; [§]The European Institute for Research and Development of Transplantation Strategies, Idar-Oberstein, Germany; [¶]Ludwig Institute for Cancer Research, Lausanne Branch, Epalinges, Switzerland, and [‖]Division of Clinical Onco-Immunology, Ludwig Institute for Cancer Research, Lausanne Branch, Hôpital Orthopédique, Lausanne, Switzerland

Received for publication October 27, 2006. Accepted for publication October 21, 2007.

The costs of publication of this article were defrayed in part by the payment of page charges. This article must therefore be hereby marked *advertisement* in accordance with 18 U.S.C. Section 1734 solely to indicate this fact.

[1] This study was supported in part by the Deutsche Forschungsgemeinschaft (SFB 432 A3), the European Commission, and the Wilhelm-Luipitz Foundation. P.R. was supported in part by a grant from the Sixth Framework Program of the European Community (Cancer Immunotherapy).

[2] Address correspondence and reprint requests to Dr. Ralf-Holger Voss, III. Medical Clinic and Polyclinic, Department of Hematology and Oncology, Johannes Gutenberg-University, Langenbeckstrasse 1, 55101 Mainz, Germany. E-mail address: hvoss@uni-mainz.de

[3] Abbreviations used in this paper: Hu, human; Cα/cα, constant domain of TCRα; Cβ/cβ, constant domain of TCRβ; GMF, geometric mean fluorescence; IMGT, ImMunoGeneTics information system; IRES, internal ribosome entry site; MDM2, mouse double minute 2; MFI, mean fluorescence intensity; Mt, mutant/mutated; RCSB, Research Collaboratory for Structural Bioinformatics, Mu, murine; TAA, tumor associated Ag; Tg, transgene; Vα or Vβ, variable domain of TCRα or TCRβ, respectively; Wt, wild type.

(19) revealed a sterically and electrostatically complementary pair of interacting residues centrally buried in the constant domains. We hypothesized that swapping their positions may favor pairing of the reciprocally mutated TCR and disfavor the formation of noncomplementary TCR chain combinations. According to ImMunoGeneTics information system (IMGT) nomenclature for the dedicated numbering of TCR constant domains (20, 21), the pair consisted of a glycine to arginine mutation at position 85.1 in the constant α (cα) domain (Gly-85.1cα-Arg) and an arginine to glycine mutation at position 88 in the constant β (cβ) domain (Arg-88cβ-Gly). Initially, the feasibility of this approach was tested for a Mu Vβ6^1 mouse MDM2(81–88) TAA-specific TCR (where Vβ is the variable β domain and MDM2 is the mouse double minute 2 oncoprotein) (3). We extended this approach to a Hu Vβ14$^+$ gp100(280–288) TAA-specific high-affinity TCR (22) and to the CD8$^+$ and CD4$^+$ subsets thereof. Structural avidity, i.e., native heterodimeric TCR$\alpha\beta$ surface expression, as well as functional avidity, i.e., cytolytic and IFN-γ-secretory effector function (23), have been assessed in retrovirally transduced bulk Hu T cells for all wild-type and mutated TCR combinations. The presence of endogenous TCR did not compromise the results, because the favored behavior of chain pairing has been reproduced in the endogenous TCR-deficient hybridoma 58α$^-$β$^-$ζ$^-$. This approach significantly inhibited the potential formation of an interspecies hybrid TCR of a mouse/human-mixed type. Tetramer dissociation experiments revealed that this molecular design did not impair recognition of the cognate Ag.

Materials and Methods

Graphic display of TCR structures and modeling

The crystal structure atom coordinates of a Mu H-2K^b-restricted TCR, 1TCR (18), and a Hu HLA-A*0201-restricted TCR, 1BD2 (19), were fetched from the Research Collaboratory for Structural Bioinformatics (RCSB) protein data bank (24) and visualized and analyzed with Swiss-PdbViewer version 3.7 (25); amino acids were mutated by taking advantage of the built-in option to browse a knowledge-based rotamer library and by adjusting the side chain dihedral angles through all empirical conformers. Atom distances, angles, and H-bond calculations have been computed and manually verified so as not to violate protein structure constraints for all modeling interventions. Human and Mu TCR structures have been visually inspected and aligned by superpositioning. For graphic illustration, solid three-dimensionally rendered protein models have been compiled in POV-Ray version 3.1g (www.povray.org/povlegal.html).

PBMC and cell lines

Bulk CD4$^+$CD8$^+$ T cells were obtained from buffy coats of Hu A2.1$^+$ donor PBMC. For this, mononuclear cells were separated by Ficoll (Biochrom) gradient centrifugation on Leucosep devices according to the manufacturer (Greiner) and cryopreserved. The Mu hybridoma 58α$^-$β$^-$CD3ζ$^-$ lacks endogenous TCRα- and TCRβ-chains and were cultured in histidinol (2 mg/ml) to sustain mouse CD3ζ expression (26).

The packaging cell lines 293T, Phoenix-Ampho (amphotropic), and Phoenix-Eco (ecotropic) were obtained from American Type Culture Collection (ATCC). They were grown in HEPES-buffered (25 mM) DMEM supplemented with 1× glutamine, 1× penicillin-streptomycin, 1× nonessential amino acids, and 10% (v/v) FCS (Cambrex) and trypsinized with 1× trypsin-EDTA (Invitrogen Life Technologies).

1.2 B α class II negative B and T lymphoblastoid hybrid (ATCC); Saos-2 clone 6 is an MDM2 transfectant (3) of the Hu HLA-A2$^-$ osteosarcoma cell line Saos-2 (ATCC); EL-3 and BV-173 (H. Stauss, Royal Free Hospital, London, U.K.) are Hu B cell precursor leukemia cell lines; IM-9 is a Hu multiple myeloma-derived, EBV-transformed B-lymphoblastoid cell line (ATCC); UoC-B1 is a class I negative early pre-B acute lymphocytic leukemia cell line (S.D. Smith, University of Chicago Medical Center, Chicago, IL). 526 mel (A2.1$^+$gp100$^+$) and 397 mel (A2.1$^+$gp100$^+$) are melanoma cell lines (M. Lotze, University of Pittsburgh, Pittsburgh, PA). Cell lines were cultured in RPMI 1640 (Cambrex) supplemented with 10% (v/v) FCS, 1× glutamine, 0.1% (v/v) gentamicin from a 50 mg/ml stock, and 0.01% (v/v) 2-ME (Sigma-Aldrich) from a 1 M stock.

Vector constructs and generation of TCR mutants

MDM2(81–88)-specific (3) and p53(264–272)-specific (4) TCR were isolated from A2-transgenic mouse spleen T cells as described elsewhere (27). The coding sequences of either TCRα and TCRβ were inserted into the multiple cloning site of the retroviral vector pBullet (13) via PCR as *NcoI*/*BamH*I-fragments. The vector was modified by inserting an internal ribosome entry site (IRES)-puromycin or IRES-neomycin cassette (Takara-Clontech) as described in Ref. 27 to enable the selection of transduced PBMC for expression of TCRα in pBullet-IRESpuro and TCRβ in pBullet-IRESneo. Amino acid replacements in the wild-type (Wt) MDM2(81–88)-specific TCR sequences were done with the mutagenic primers 5′-gatcca agagcaatagggccattgccctggagc-3′ and 5′-tactgcctgagcaggcgccatgagggtctctgct-3′ and their complementary counterparts to yield Gly-85.1cα-Arg in Mu TCRα and Arg-88cβ-Gly in TCRβ, respectively, using the QuikChange site-directed mutagenesis kit (Stratagene). For the chimeric TCR MDM2 and full-length Hu TCR gp100, the mutagenic primers 5′-gacttcaagagcaac agagctgtggcctggagc-3′ and 5′-tactgcctgagcaggcgctgaggggtctggagc-3′ yielded the reciprocal Ser-85.1cα-Arg and Arg-88cβ-Gly mutants. Nomenclature of the mouse and human Cα/Cβ was adopted from IMGT (20, 21).

Retroviral transduction and drug selection

The protocol of G. P. Nolan's laboratory (28) was slightly modified as described in detail elsewhere (27). Selection of TCRβ$^+$-transduced T cells was achieved by adding neomycin at a final concentration of 800 μg/ml (Invitrogen Life Technologies) for 7 days, and the selection of TCRα$^+$-transduced T cells was accomplished by adding puromycin (Sigma-Aldrich) at a final concentration of 5 μg/ml for 2 days to RPMI 1640 medium supplemented with Hu AB serum. Surviving bulk T cells were cultured for at least 1 wk with CD3/CD28 labeled magnetic beads (Dynabeads; Invitrogen-Dynal) and 40–100 U of IL-2 (Proleukin, Chiron) before transgene expression and function analysis. For transduction of a Mu hybridoma, Phoenix-Eco and the amphotropic envelope vesicular stomatitis virus glycoprotein were used. TCR-introduced 58α$^-$β$^-$CD3ζ$^+$ needed selection in 2 mg/ml neomycin (6 days) followed by 5 μg/ml puromycin (2 days) as estimated from killing dose responses. Homogenous, untouched CD4$^+$ T cell subset was isolated by depletion of the CD8$^+$ T cells using anti-CD8$^+$ Ab-labeled magnetic beads (Miltenyi-Biotec).

Flow cytometric analysis and evaluation

Data acquisition was performed on an EPICS ALTRA HyPerSort (Beckman Coulter) or a FACSCalibur (BD Biosciences) device, and raw data analysis was conducted with the Expo32 software (Beckman Coulter). T cells were sorted on FACSAria (BD Biosciences). Human T cells were stained with anti-Mu Vβ6-FITC/PE (BD Biosciences), anti-Hu TCRαβ-PE (Beckman Coulter), anti-Hu Vβ14-PE (Beckman Coulter), anti-Hu CD8-PC5, and anti-Hu CD4-FITC (Beckman Coulter) Ab. MDM2(81–88)-PE- and gp100(280–288)-PE-specific tetramers (0.4 mg/ml) were synthesized as published elsewhere (29). Tetramers (0.5 μl) were added to 0.1×10^6 T cells in 50 μl (~0.4 μg/ml) for 45 min at 8°C.

Chromium-release assay

Transduced T cells were assayed in a 4-h ^{51}Cr-release assay at various E:T ratios for lytic activity against TAP-deficient T2, with or without antigenic peptide, or tumor cell lines (2). To correct for varying TCR expression and size of CD8$^+$ population in retrovirally transduced bulk Hu T cells, Vβ6$^+$CD8$^+$:T and gp100 tetramer$^+$CD8$^+$:T ratios, respectively, were calculated from contemporary flow cytometry analysis (3). EC_{50} as a measure of the ligand concentration yielding half-maximal lysis was calculated from peptide titration cytotoxicity experiments and dose-response sigmoidal regression analysis according to $Y = Top/(1 + 10^{\wedge}((logEC_{50}-X)))$ with GraphPad Prism version 3.0 software.

Competitive tetramer dissociation assay

The experiments were performed at 4°C to increase cell viability and minimize residual tetramer binding due to capping and tetramer internalization (30). The protocol was as outlined in Ref.31 using a FITC-labeled anti-Vβ6 Ab as competitor. Briefly, 10×10^6 TCR-introduced T cells were stained in a volume of 2500 μl with 25 μl of PE-Cy5 (PC5)-labeled tetramer (0.4 μg/ml) at 4°C for 45 min in the presence of 0.5% sodium azide to reduce the internalization of TCR/tetramer complexes. All subsequent steps were performed in the presence of NaN_3. After washing two times with ice-cold PBS, the T cells were sorted on a FACSAria device (BD Biosciences) to equal and high tetramer geometric mean fluorescence (GMF) intensities for different TCR-transduced T cell populations. Sorted and viable T cells (0.5×10^6) were resuspended in 150 μl and tetramer dissociation was initiated by the addition of 12.5 μl (0.5 mg/ml) Vβ6 Ab.

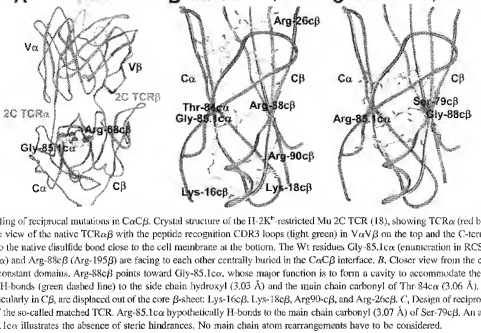

FIGURE 1. Modeling of reciprocal mutations in Cα*C*β. Crystal structure of the IE-2K^{k}-restricted Mu 2C TCR (18), showing TCRα (red backbone) and TCRβ (blue). *A*, Overall side view of the native TCRα*β* with the peptide recognition CDR3 loops (light green) in V*α*V*β* on the top and the C-termini of C*α*C*β* at the −1 position relative to the native disulfide bond close to the cell membrane at the bottom. The Wt residues Gly-85.1cα (enumeration in RCSB protein data bank entry 1TCR: Gly-179α) and Arg-88cβ (Arg-195β) are facing to each other centrally buried in the C*α*C*β* interface. *B*, Closer view from the cell membrane to the core interface of the constant domains. Arg-88cβ points toward Gly-85.1cα, whose major function is to form a cavity to accommodate the bulky side chain of Arg-88cβ. Arg-88cβ H-bonds (green dashed line) to the side chain hydroxyl (3.03 Å) and the main chain carbonyl of Thr-84cα (3.06 Å). All other bulky and charged residues, particularly in C*β*, are displaced out of the core β-sheet: Lys-16cβ, Lys-18cβ, Arg90-cβ, and Arg-26cβ. *C*, Design of reciprocal complementarity into the contact site of the so-called matched TCR. Arg-85.1cα hypothetically H-bonds to the main chain carbonyl (3.07 Å) of Ser-79cβ. An atomic sphere of 5-Å radius around Arg-85.1cα illustrates the absence of steric hindrances. No main chain atom rearrangements have to be considered.

As a control, 0.2×10^6 bulk Wt TCR MDM2-transduced T cells were stained with an irrelevant gp100(280–288)-PC5-specific tetramer displaying a very low signal over time. Twelve aliquots each corresponding to 40,000 cells were withdrawn between 0 min, i.e., before competitor addition, and 1–90 min after addition and immediately pipetted into ice-cold paraformaldehyde-containing PBS (1%; w/v) to stop the reaction. Three thousand viable cells were gated and analyzed for residual tetramer binding on a FACSCalibur flow cytometer (BD Biosciences). Processing of GMF intensities were done with GraphPad Prism version 3.0 software.

Results

Designing reciprocal complementarity at the Cαβ interface in Mu TCR

To favor the interaction of introduced TCRα- and TCRβ-chains in Hu T cells, we focused on the C*α*C*β* interface in the associated TCR heterodimer. We used as model the crystal structure of the Mu 2C TCR (Ref. 18 and the RCSB protein data bank). We concentrated on the invariant constant domains so as to generalize the approach to the majority of TCR subfamilies. This is particularly relevant for the transduction of bulk T cell populations, as this is the favorable setting in a clinically adoptive transfer protocol. A successful strategy was the reciprocal substitution of two facing residues, differing in size, to yield sterically complementary "knob-into-hole" mutations as previously shown for Abs (32). However, a characteristic of the TCR structure is the pronounced charge asymmetry between the C*α*- and C*β*-domains (18). Because electrostatic forces exert a long-ranging effect in protein structures (33), we hypothesized that the combined reciprocal substitution of both side chain volume and charge would enhance preferential TCR chain pairing.

The TCR C*α*- and C*β*-domains were structurally related (Fig. 1*A*). The *β*-sheets comprising *β*-strands ABED of each domain were juxtaposed to each other while the *β*-sheets GFC were staggered behind. According to IMGT numbering, a pair of interacting residues, Arg-88 in the constant domain of TCR*β* (Arg-88c*β*) and Gly-85.1 in the constant domain of TCR*α* (Gly-85.1c*α*), turned out to be candidate residues for reciprocal exchange (Fig. 1*B*). They were both located midway in the inner *β*-strand E of their respective C-domain. The Arg-88c*β* side chain centrally protrudes from its twisted *β*-sheet and points to Gly-85.1c*α*, which is nested at the base of its concave-shaped *β*-sheet.

The C*α*C*β* interface was endowed with polar amino acids, hydrophobic patches, and a skewed distribution of acidic residues in C*α* and basic residues in C*β*. The side chain of Arg-88c*β* was stacked between the hydrophobic residues Leu-24cα (strand B), Leu-84.2cα (strand D), Ile-86cα (strand E),Val-22cβ (strand B), and partly Arg-90cβ (strand E). Arg-88cβ was not thoroughly in a *trans* conformation because the dihedrals χ_1, χ_2, and χ_4 equal −73.8°, −63.3° and 149°, respectively, so as not to conflict with the opposite *β*-strand E of C*α*. The positively charged guanidinium group of Arg-88c*β* did not form a salt bridge but was predominantly surrounded by polar residues.

The reciprocal substitutions Gly-85.1cα→Arg-85.1cα and Arg-88cβ→Gly-88cβ (Fig. 1*C*) elicited no steric hindrance for that particular arginine conformer available from the empirical database in the Swiss-PdbViewer (χ_{1-5} = −175°, −175°, 71.1°, 176°, and 179.9°) that yielded the lowest score for steric distortion. Although the charged guanidinium group was slightly shifted toward the C*β* domain, the Arg-85.1c*α* mutant is predicted to be similarly stacked between the same hydrophobic residues such as in the Wt. Correspondingly, interactions of the guanidinium group were restricted to polar residues. However, the empirical structure of the Arg-85.1c*α* conformer was not available from crystallization and x-ray diffraction analysis. In 2C TCR, the coordination of water molecules at the interface, such as H_2O 15 centered between Wt Arg-88c*β* and Arg-90c*β*, indicated hydrophilic accessibility and allowed some stereochemical freedom, although low temperature factors for Arg-88c*β* (C*δ*: 24.07 Å^2) and its proximate residues predicted a rather rigid structure.

From a structural point of view, we hypothesized a positive effect on chain pairing for the prominent Arg-88c*β* in analogy to binding "hot spots" that dictate the association of proteins by contributing substantially to the binding free energy (34). Human TCR bear also a small residue, Ser-85.1cα, and large residue, Arg-88c*β*, as a consequence of the high homology in primary and tertiary structure. This may suggest a species-independent generalization of our approach.

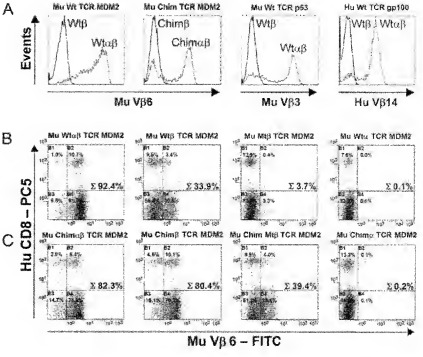

FIGURE 2. Single TCRβ vs heterodimeric TCR$\alpha\beta$ surface expression. Flow cytometry analysis of retrovirally transduced and antibiotic-selected Mu hybridoma 58$\alpha^-\beta^-$CD3ζ^- (*A*) or bulk Hu T cells (*B* and *C*). The Wt or Mt TCR constructs of Mu or Hu origin comprised both or merely the single TCRα- or TCRβ-chain as indicated from *left* to *right*: *A*, Overlay histogram for surface expression of a heterodimeric Mu Wt MDM2(81–88)-specific TCR, its partially humanized (Chim, chimeric) construct, a Mu Wt p53(264–272)-specific and a Hu Wt gp100(280–288)-specific TCR (dotted line) vs that of the corresponding single TCRβ-chain (bold line). *B*, Dot plots for surface expression of introduced TCRβ in the CD4$^-$CD8$^+$ subsets of PBMC monitored by anti-Hu CD8 and anti-Mu Vβ6. It aligns from *left* to *right* the heterodimeric Mu Wt MDM2(81–88)-specific TCR, its single TCRβ, a point-mutated TCRβ (Arg-88cβ-Gly; Fig. 1), and a single TCRα as negative control. *C*, As in *B*, but documents the expression of the partially humanized TCR in CαCβ.

Introduced TCRβ needed heterodimerization to TCRα for export to the cell surface

Initially, we needed an assay to determine the impact that the mutations would have on TCR chain pairing. For this, we assessed whether surface expression of the introduced TCR β-chain served as a readout for effective chain pairing of either the introduced TCR α- and β-chains among themselves or a single introduced TCR β-chain with an arbitrarily endogenous TCRα counterpart to form a hybrid TCR (11). The rationale was that pairing stabilizes the TCR and subsequently promotes its integration into the multimeric CD3 complex as a prerequisite for export to the cell membrane. The TCRα could not be assessed due to the lack of Abs. Moreover, a construct with an octamer histidine tag in front of the variable domain failed to allow flow cytometric identification of surface TCRα (data not shown). Introduced TCRβ were monitored with subfamily-specific Abs. The presence of both Ag-specific TCRα and TCRβ was detected with soluble fluorescent tetramer molecules, that are composed of streptavidin/biotin-linked TAA peptide/HLA-A2 multimers (29). But, as shown below, the correlation of tetramer with Vβ-14, Vβ-6, and Vβ-3 staining for native TCR specific for a gp100, MDM2, or p53 Ag justified the use of Vβ-specific Abs to estimate heterodimeric TCR$\alpha\beta$ expression (Figs. 2*A* vs 3*A* and 4*A* vs 4*B*; data not shown).

First, we tested this approach in the hybridoma 58$\alpha^-\beta^-$CD3ζ^- devoid of endogenous TCR (26). Because CD3ζ is the major functional component of the CD3 complex (35), this cell line was stably transfected with the cDNA encoding the homodimer to shuttle TCR export.

Different tumor-specific TCR originated from a Mu Wt or a chimeric TCR; i.e., in the constant domains C$\alpha\beta$ humanized MDM2(81–88)-specific TCR (Mu Wt TCR MDM2 or Mu chimeric TCR MDM2; Ref. 3), a Mu p53(264–272)-specific TCR (Mu Wt TCR p53; Ref. 4), and a Hu gp100(280–288)-specific TCR (Hu Wt TCR gp100; Ref. 22) were expressed either as double chain TCR$\alpha\beta$ or as single TCR β-chains. For the latter one, the missing plasmid encoding TCRα was replaced by the empty vector pBullet-IRESpuromycin. Transfectants were selected with the appropriate antibiotics (see *Materials and Methods* and Fig. 2*A*). Thus, introduced TCR$\alpha\beta$ expression follows a Gaussian-like random distribution on hybridoma and bulk T cell cultures. Essentially, in all cases the TCR β-chain could be detected at the cell surface by FACS analysis only when TCRα was coexpressed. Likewise, we observed tetramer binding only for the heterodimeric Hu TCR gp100 in hybridoma, proving that the pairing of TCRα with TCRβ is a necessity for TCR export (see Fig. 3*A*). Noteworthy, the Hu TCR was able to associate with Mu CD3ζ. Tetramer staining of a CD8-deficient hybridoma succeeded only for introduced CD8-independent TCR such as TCR gp100 and p53, not for the CD8-dependent TCR MDM2.

Point mutations at the interface of TCRβ affected export to the T cell surface

Next, we examined the chain pairing of introduced TCR chains in antibiotic-selected bulk Hu T cells. We anticipated that retrovirally transduced Mu and even more Hu TCR chains were able to interact with endogenous TCR. As opposed to the hybridoma model (Fig. 2*A*), the pairing of TCRβ with any endogenous TCRα should rescue its surface expression. The point mutation candidate Arg-88c$\beta\rightarrow$Gly-88cβ in TCRβ was expected to be poorly expressed in the absence of its complementary TCRα counterpart in Hu T cells. We tested this concept with the Wt and partially humanized MDM2-specific TCR. We observed a marked expression for the heterodimeric Wt TCR MDM2 irrespective of the CD4$^-$CD8$^+$ T cell subset (92.4%; Fig. 2*B*). Reduction of Vβ6 positivity for chimeric TCR MDM2 (82.3%; Fig. 2*C*) was probably due to some structural instability of the chimerized elbow region. Although Wt TCRβ expression was substantially reduced in the absence of its TCRα (drop from 92.4 to 33.9%), transduction of the single chimeric TCR β-chain construct resulted in expression at a level as high as that of the heterodimeric TCR (82.3 to 80.4%). This may be explained by its higher propensity to associate with endogenous Hu TCRα. The residual Vβ6 staining for single Wt TCRβ reflected some competence to bind to Hu TCR. Eventually, as already shown for the

hybridoma model (Fig. 2*A*), coexpression of TCRα seemed to support pairing and recovery of TCRβ at the cell surface.

Replacement of Arg-88cβ for Gly-88cβ to generate a TCRβ mutant unmatched to endogenous TCR α-chains abolished surface expression (Fig. 2*B*, from 33.9 to 3.7%) and substantially diminished that of the single chimeric TCRβ mutant (Fig. 2*C*, from 80.4 to 39.4%). The higher residual Vβ6 positivity (39.4% vs 3.7%) was explained by the higher potency of a Hu TCRβ C-domain to pair with its endogenous counterparts and thus compensates for the local residue mismatch.

It was highly unlikely that the reduced staining of the TCRβ mutants was merely an artifact of a disabled recognition by the Vβ6 Ab, because the mutation and the epitope were distantly located in different domains. Furthermore, chimerization to a Hu constant domain preserved Vβ6 staining (Fig. 2, *B* and *C*; Mu Wt TCR MDM2 vs Mu chimeric TCR MDM2). Additionally, a decrease in surface expression correlated with an increase in cytoplasmic detection (data not shown). However, the total intracellular recovery was decreased for the TCRβ mutants, indicating an increased instability of those unmatched and therefore largely unpaired chains. Collectively, TCR Vβ6 staining closely reflected TCR surface expression on $CD8^+$ and $CD4^+$ T cell subsets and thus proposes a mechanism for TCR export depending on effective chain pairing.

Reciprocal mutations in CαCβ of introduced TCR restored surface expression in hybridoma

The results from Fig. 2 suggested, that the rebuilding of complementarity at the interface of TCR$\alpha\beta$ would restore surface expression. Mutant TCR bearing the reciprocal mutations as described in Fig. 1 were coexpressed after drug selection in hybridoma $58\alpha^-\beta^-CD3\zeta^-$ in the absence of endogenous TCR. As opposed to the CD8-dependent TCR MDM2, the presence of both TCRα and TCRβ of the gp100-specific TCR was detectable via tetramer staining in a CD8-deficient hybridoma. Hence, we chose the Hu TCR gp100 to study the combinations of Wt and mutated (Mt) chains of its own species (Fig. 3*A*). Wt TCR gp100 achieved the highest expression when quantified by a tetramer (mean fluorescence intensity (MFI) 29.2), followed by the reciprocally mutated TCR (also referred to as matched TCR; i.e., Arg-85.1cα/Gly-88cβ, MFI 6.5). Both unmatched Mtα/Wtβ (i.e., Arg-85.1cα/Arg-88cβ; MFI 0.3) and Wtα/Mtβ (i.e., Ser-85.1cα/Gly-88cβ; MFI 2.9) TCR combinations substantially decreased in surface expression (Fig. 3*A*). The same ranking was observed for a Vβ14-staining (data not shown). The presence of two bulky and charged arginine residues that triggered steric hindrance and electrostatic repulsion seemed to be more detrimental to chain association than that of small and neutral residues, which led to withdrawal of steric complementarity and charge.

The formation of hybrid TCR of an interspecies mouse/human-mixed type does occur

The generation of a novel high-affinity, tumor-specific TCR in an A2-Tg mouse model (3, 4) necessitated us to assess the propensity of Mu TCR chains to interact with Hu TCR. Human TCR gp100 was combined with murine TCR MDM2 chains to yield a Hu/Mu mixed type (Fig. 3, *B* and *C*). Monitoring the surface expression of Hu TCRβ (Fig. 3*B*, Hu Vβ14) allowed us to indirectly quantify the interaction of Mu TCRα with Hu TCRβ, while monitoring Mu TCRβ (Fig. 3*C*; Mu Vβ6) allowed us to directly quantify the interaction of Mu TCRβ with Hu TCRα. In either setting, interspecies Wt TCR combinations displayed a strong propensity to heterodimerize (dark gray-shaded histograms in Fig. 3: MFI 21.5 for Mu Wtα MDM2/Hu Wtβ gp100 and 18.4 for Hu Wtα gp100/Mu Wtβ MDM2) somewhat behind that of the related intraspecies Wt

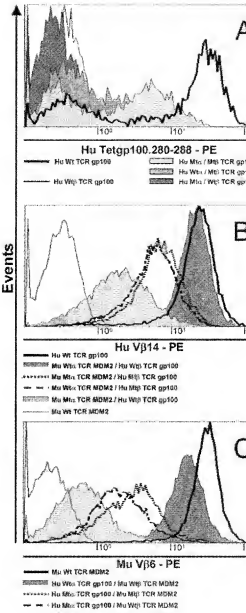

FIGURE 3. Surface expression for intraspecies and interspecies $\alpha\beta$-chain combinations of Wt, matched, or unmatched TCR in transduced and drug-selected hybridoma $58\alpha^-\beta^-CD3\zeta^+$. *A*, Overlay histograms of tetramer-labeling intensities of intraspecies combinations of a native (bold line), matched Mtα/Mtβ (shaded light gray), unmatched Wtα/Mtβ (shaded gray), or Mtα/Wtβ (shaded dark gray) TCR gp100 and its single TCRβ-chain (thin line). Human Wt TCR as opposed to Mu TCR bears a serine instead of a glycine at position 85.1cα. *B* and *C*, Interspecies combinations of individual Mu MDM2(81–88)-specific and Hu gp100(280–288)-specific TCR chains monitored either by Hu Vβ14 positivity (*B*) or Mu Vβ6 positivity (*C*). In *B* and *C*, relevant native TCR is denoted by a bold line, irrelevant native TCR by a thin line, species-mixed Wtα/Wtβ TCR by dark gray shading, and mixed Mtα/Mtβ TCR by a dotted line. For the unmatched pairs in *B*, mixed Mu Mtα/Hu Wtβ TCR is denoted by light gray shading and Mu Wtα/Hu Mtβ TCR by a dashed line. In *C*, mixed Hu Wtα/Mu Mtβ TCR is denoted by light gray shading and Hu Mtα/Mu Wtβ TCR by a dashed line. The shift of the shaded curves in *B* and *C* illustrate the designated effect of TCR chain uncoupling that the single mutations have on mixed or so-called hybrid TCR.

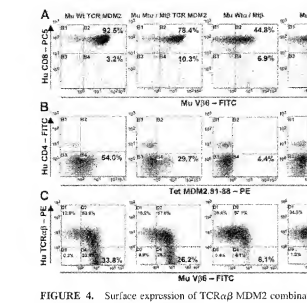

FIGURE 4. Surface expression of TCR$\alpha\beta$ MDM2 combinations in Hu T cells. Dot plot FACS-analysis of transduced and drug-selected bulk Hu T cells with all Mu TCR MDM2 combinations as follows from *left* to *right*: TCR bearing the Wt α- and β-chain, TCR bearing the mutations of reciprocal complementarity (matched Mtα/Mtβ TCR), Wt TCRα-chain combined with TCRβ harboring Arg-88cβ-Gly (unmatched Wtα/Mtβ TCR), and the mutated Gly-85.1cα-Arg TCRα-chain combined with Wt TCRβ (unmatched Mtα/Wtβ TCR). *A*, Surface expression of the introduced TCRβ-chain is illustrated using the subfamily-specific Ab Mu Vβ6. *B*, The percentage of $CD8^+$ MDM2(81–88) tetramer (Tet)-positive T cells representative of TCR$\alpha\beta$ with structural integrity. *C*, The down-regulation of bulk endogenous TCR triggered by introduced Mu TCR MDM2 is documented by using an anti-Hu TCR$\alpha\beta$ Ab.

TCR (bold lines: MFI 25.2 in Fig. 3*B* and 33.4 in Fig. 3*C*). Interspecies TCR are able to interact, at least for the Hu Vα8/Mu Vβ6 and Mu Vα10/Hu Vβ14-subfamily combinations examined here, and may also take place in Hu PBMC as a disfavored side reaction. Importantly, either one of the unmatched combinations of a Mu Mtα- or Mtβ-chain with a Hu Wt counterpart were substantially reduced in surface expression (light gray-shaded histograms: MFI 2.8 for Mu Mtα MDM2/Hu Wtβ gp100 in Fig. 3*B* and MFI 1.0 for Hu Wtα gp100/Mu Mtβ MDM2 in Fig. 3*C*). The reciprocal mutations also tended to restore pairing of interspecies-matched TCR (dotted lines) better than the single mutation of the other Mu Wt/Hu Mt unmatched TCR (dashed lines). Although the latter TCR combinations do not have any relevance for gene therapy, this result in principle may argue for the envisaged structural manipulation. Thus, a single residue substitution on either side of the Mu CαCβ interface disfavors, as designated, the pairing of introduced and endogenous TCR and may diminish the formation of hybrid TCR.

Reciprocal mutations in introduced Mu TCR MDM2 restored structural avidity in Hu T cells

All intraspecies combinations of wild type and mutant Mu TCR MDM2 were then analyzed in antibiotic-selected bulk Hu PBMC (Fig. 4) where endogenous TCR might interfere with chain pairing. First, we stained for V$\beta6^-$ as a surrogate for overall TCR expression (Fig. 4*A*). The frequency of Wt TCR MDM2-positive T cells was high for both the larger $CD8^+$ (92.5%) and the smaller $CD4^+$ (3.2%) T cell subsets, whereas introducing a single mutation as outlined previously in either TCRα (Mtα/Wtβ) or TCRβ (Wtα/Mtβ) decreased the surface density of TCR. Because the single Wt or Mt β-chain (Wtβ and Mtβ) only elicited TCR V$\beta6^+$ in a minor fraction of T cells (Fig. 2*B*), the observed en bloc Vβ6 positivity for unmatched Mtα/Wtβ TCR MDM2 (52.7% for $CD8^+$ and 6.4% for $CD4^+$) or Wtα/Mtβ

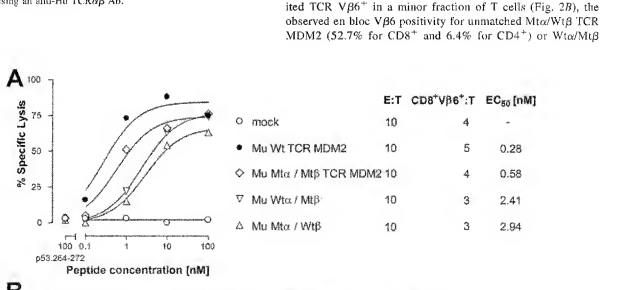

FIGURE 5. Chromium-release assay for transduced and drug-selected bulk Hu T cells with all Wt and Mt Mu TCR$\alpha\beta$ MDM2 combinations as explained in the legend to Fig. 4. *A*, ○, Mock; ●, Wt TCR, ◇, Mt/Mtβ, ▽, Wtα/Mtβ; △, Mtα/Wtβ. Cytolytic efficiency toward MDM2(81–88) peptide-pulsed T2 cells is shown for an E:T ratio of 10:1 and corrected to $CD8^+V\beta6^+$:T ratios (see *Materials and Methods*). EC_{50} values were calculated from sigmoidal curve fitting. *B*, Cytolytic efficiency toward tumor cell lines. ○, EU-3; □, BV-173; ◇, IM-9; ●, UoC-B1 as HLA-A2.1$^-$ control; ▽, Saos-2; △, Saos-2 clone 6

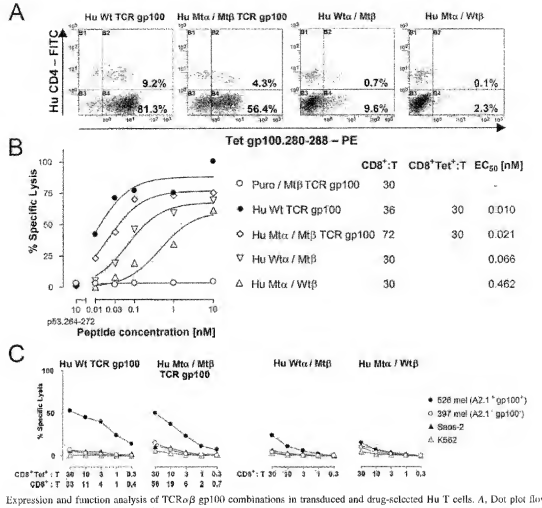

FIGURE 6. Expression and function analysis of TCR$\alpha\beta$ gp100 combinations in transduced and drug-selected Hu T cells. *A*, Dot plot flow cytometry analysis of bulk Hu T cells with all Hu TCR gp100 combinations in analogy to TCR MDM2 as described in the legend to Fig. 4. Both $CD4^+$ and $CD8^+$ subsets are tetramer (Tet) positive, indicative of a CD8-independent TCR. *B*, Peptide titration in chromium-release assays for TCR gp100 combinations. ○, TCRβ; ●, Wt TCR; ◇, Mtα/Mtβ; ▽, Wtα/Mtβ; △, Mtα/Wtβ. *C*, Cytolytic efficiency toward the Hu $A2.1^+$ melanoma cell line 526 (●) and the $A2.1^-$ melanoma cell line 397(○), $gp100^-$ Saos-2(▲), and the NK target K562(△) as negative control. E:T ratios are based on $CD8^+$:T or $CD8^+$gp100 $tetramer^+$:T ratio ($CD8^+Tet^+$:T) in case of discernible tetramer staining (*A*).

(44.8 and 6.9%) was likely due to residual interaction with the introduced counterpart. T cells transduced with the matched Mtα/Mtβ TCR MDM2 exhibited a significant recovery of Vβ6 positivity (78.4 and 10.3%), indicative of the restoration of steric and electrostatic complementarity. Conclusively, Hu endogenous TCR did not counteract the desirable effect of preferential chain pairing despite a pronounced propensity for interspecies hybrid TCR formation (Fig. 3, *B* and *C*).

A more comprehensive readout for functional TCR expression was provided by tetramer staining, because HLA-A2 binding requires the dual presence of TCRα and TCRβ in a native conformation and thus gives an estimate for structural avidity (Fig. 4*B* and Ref. 23). The unmatched TCR pairs failed to confer tetramer staining (4.4 and 2.6%, respectively). In contrast, the results from Fig. 4*A* indicated a gradual decline for the unmatched TCR, implying that expression of heterodimeric TCR with improper structure at their interface was not abolished but had an severe impact on Ag recognition. Most importantly, coexpression of the complementary TCR chain pair restored tetramer positivity and hence structural integrity to more than one-half of that of the Wt TCR (29.7 vs 54%). In general, we did not observe >70% tetramer-positive $CD8^+$ T cells for the CD8-dependent Wt TCR MDM2 in any experiment (4).

Introduced TCR have to compete with endogenous TCR for integration into the CD3 complex (11). Retroviral overexpression and favorable pairing of Mu TCR among themselves promoted their incorporation into the signaling machinery and the down-regulation of endogenous TCR on the cell surface of Hu T cells (16, 17). The amount of introduced TCR-dependent down-regulation of endogenous TCR correlated with the competitive strength and stability of a particular introduced TCR construct (Fig. 4*C*). The unmatched TCR did not suppress endogenous TCR (6.1 and 10.1%) as opposed to the matched TCR. From flow cytometry analysis, apparently 26.2% of the T cells have lost endogenous TCR surface expression. With respect to its diminished Vβ6 positivity ($CD8^+$ and $CD4^+$: 88.7 vs 95.7%; Fig. 4*A*) this is in line with a higher competitive strength for Wt TCR MDM2 (33.8%. Fig. 4*C*). Successful pairing corresponded to introduced TCR surface expression and inversely related to endogenous TCR recovery. This equally applied to $CD8^+$ and $CD4^+$ T cell subsets (not shown).

These differences in the cellular phenotype were not caused by genetic modifications at the RNA level. Semiquantitative RT-PCR according to (36) demonstrated the equal abundance of mRNA for all TCR combinations (data not shown). Furthermore, intracellular

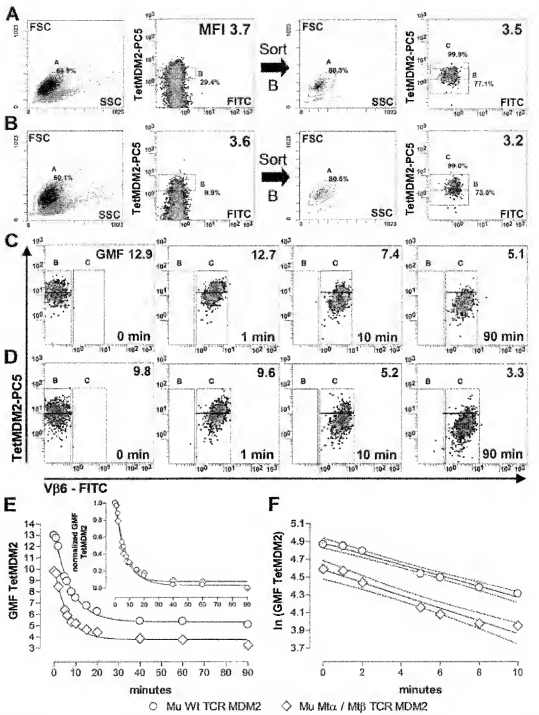

FIGURE 7. Half-lives of competitive tetramer dissociation for Wt and matched TCR MDM2 were indistinguishable. *A* and *B*, $CD8^+$ Mu Wt TCR MDM2 (*A*, *C*, *E*, and *F*)-introduced or Mu Mtα/Mtβ TCR MDM2 (*B*, *D*, *E*, and *F*)-introduced T cells were stained with tetramer (TetMDM2-PC5) and were sorted on a FACSAria flow cytometer (BD Biosciences) to equal and high fluorescence intensities (gate B in the *left-hand* density plot). All incubations were done in the presence of 0.5% NaN_3 to minimize tetramer-complexed TCR internalization and cell toxicity (*left-hand* forward scatter (FSC)/side scatter (SSC) dot plot). Reanalysis of the sorted cells demonstrated a reasonable 80% survival (*right-hand* scatter dot plot) and almost equal tetramer signal intensity (*right-hand* density plot: MFI 3.5 and 3.2, respectively). Bound tetramer dissociated somewhat during sample preparation as shown by the modest shift out of gate B, *C* and *D*. Sorted T cells were submitted to Vβ6 Ab-mediated competition immediately after sorting. *Inset* numbers give GMF intensities of tetramer signals (*upper right*) for gates B or C, and time intervals in minutes (*lower right*). For clarity, decrease of GMF intensities are only shown for 0 min, i.e., before competitor addition, and 1, 10, and 90 min after addition. A horizontal black bar inside gates B or C refers to GMF for $t = 0$ min and helps visualize the subsequent tetramer decay. *E*, Chart of tetramer dissociation over time for Mu Wt TCR MDM2 (○) and the matched TCR MDM2 (◇). GMF intensities were submitted to nonlinear regression using a one-phase exponential decay equation. The *inset* demonstrates a closely related tetramer dissociation for the normalized data. *F*, Due to residual tetramer internalization, a more reliable evaluation of tetramer decay kinetic is confined to the initial 10 min (3); the runs test confirms a linear relationship for both TCR ($p = 0.5$ and 0.2, respectively). The related half-lives equal ln2/slope; $t_{1/2} = 11.4 \pm 0.7$ min and $t_{1/2} = 9.6 \pm 0.8$ min. The difference of their slopes was statistically not significant ($p = 0.2$, according to GraphPad Prism version 3.0 software). The 95% confidence intervals (curved dashed lines) support this notion.

staining demonstrated an almost equivalent TCR distribution indicative for comparable protein translation.

Reciprocal mutations in Mu TCR MDM2 restored functional avidity in Hu T cells

The functional avidity of transduced T cells was determined in chromium-release assays on targets sensitized with decreasing amounts of the antigenic peptide (Fig. 5*A*). T cells transduced with the matched TCR were almost as efficient as those transduced with the Wt TCR; EC_{50} values were 0.28 nM for the Wt TCR and 0.58 nM for the matched Mtα/Mtβ TCR. T cells transduced with the unmatched TCR displayed a 10-fold reduction in functional avidity (2.94 nM for Mtα/Wtβ TCR and 2.41 nM for Wtα/Mtβ). Interestingly, the lower but still detectable cytolytic efficacy did not correspond to the lack of tetramer staining (Fig. 4*B*). However, this is in line with other reports (23).

Subsequently, the ability of transduced T cells to recognize and lyse target cells presenting naturally processed MDM2(81–88) peptide was determined (Fig. 5*B* and Ref. 3). An MDM2 transfectant of the osteosarcoma Saos-2 was efficiently recognized by T cells transduced with the Wt TCR (82% for a corrected E:T ratio of 5 for $CD8^+V\beta6^+$-T) and, to a lower extent, by T cells expressing the matched TCR (52% for $CD8^+V\beta6^+$-T = 4). Accordingly, the tumor cell lines EU-3, IM-9, and BV-173 were lysed more efficiently by the Wt than by the matched TCR MDM2 (45/28% for $CD8^+V\beta6^+$-T = 15/13). T cells transduced with the unmatched TCR pair did not detectably recognize any target cell line.

Reciprocal mutations in Hu TCR gp100 restored structural and functional avidity in Hu T cells

Analogous to the experiments performed with the Mu MDM2-specific TCR, we determined the function of a high-affinity Hu gp100(280–288)-specific TCR and its mutants bearing the same design of reciprocal mutations, Ser-85.1cα-Arg and Arg-88cβ-Gly (Fig. 6). More likely than Mu TCR, the Hu TCR will form a hybrid TCR with endogenous TCR that would be counterproductive to the aim of preferential pairing. As shown before for a partially humanized TCR MDM2 (Fig. 2*C*), the weakening of the interface interaction by the mutation Gly-88cβ seemed to be vastly antagonized by the multitude of interactions along the large C-domain's surface area. Despite this, the matched TCR yielded more than one-half of the Wt tetramer positivity for the $CD8^+$ T cell subset (56.4 vs 81.3%; Fig. 6*A*) while the unmatched TCR failed (9.6 and 2.3%). This could also be demonstrated for the TCR gp100-transduced as opposed to the TCR MDM2-transduced $CD4^+$ T cell subset (Fig. 4*B*).

Next, peptide titration was performed for all Wt and mutant TCR combinations (Fig. 6*B*). Although the EC_{50} value of the Wt TCR (0.01 nM) was 28-fold lower than that of the Mu Wt TCR MDM2, the reduction in cytolytic efficiency for all mutant TCR (Mtα/Mtβ TCR gp100, factor 2.1; Wtα/Mtβ, factor 6.6; Mtα/Wtβ, factor 46) followed the same order and roughly the same range. Again, unmatched TCR were predominantly affected. Mtα/Wtβ TCR gp100 was particularly compromised in function. In the native structure Ser-85.1cα contributes with a polar side chain interaction in contrast to a glycine in Mu TCR. When mutated to charged Arg-85.1cα, it may more severely distort protein structure. This corresponded to the weakest structural avidity (Fig. 6*A*). Substantial recognition of an $A2^+gp100^+$ melanoma was apparent with only the Wt and matched TCR (Fig. 6*C*).

IFN-γ cytokine secretion was tested by ELISPOT analysis for a homogenous $CD4^+$ population. Again, recognition of gp100(280–288)-pulsed T2 was accomplished down to the nanomolar range exclusively for the Wt and matched TCR (data not shown). Collectively, the reciprocal mutations affected structural and functional avidity equally for both the $CD8^+$ and $CD4^+$ T cell subsets. The feasibility of the reciprocal mutation concept was proven for a Hu tumor-reactive TCR despite a putatively higher propensity to form hybrid TCR.

Reciprocal mutations did not affect molecular recognition of Ag

There are several lines of evidence indicating that dissociation rates rather than equilibrium binding to peptide/MHC ligands reflect the functional avidity of T cells (37, 38). First-order dissociation kinetics were accomplished for Wt and reciprocally mutated TCR MDM2 by anti-TCR (Vβ6-antibody (Fig. 7) in analogy to Ref. 31)- or anti-class I (Ref. 39 and data not shown)-based competition to tetramer-saturated T cells. To yield comparable introduced TCR surface densities, we stained bulk T cells with the MDM2(81–88)-specific tetramer on a preparative scale and sorted them for equal and high MFI (Fig. 7, *A* and *B*). Spontaneous tetramer dissociation after sorting (Fig. 7, *A* vs *B*) and washing (Fig. 7, *C* vs *D*) may account for the slight differences in their MFI values. Nevertheless, sorting greatly improved the normalization of the tetramer signal when compared with TCR MDM2-transduced bulk T cell populations (Figs. 4*B* and 7, *A* vs *B*). Because rapid tetramer internalization (30) deprives the competitor of the accessible TCR on the cell surface, we initially observed competition efficiencies of at best 50% (not shown). We then determined 0.5% sodium azide as an optimal concentration to combine reduced tetramer internalization with low cell toxicity (Fig. 7, *A* and *B*). The kinetic analysis revealed a very similar dissociation for both TCR constructs (Fig. 7, *C* and *D*) that proved to be nearly indistinguishable after nonlinear regression (Fig. 7*E*). Transformation of the GMF intensities to the natural logarithm (39) revealed a substantial nonlinear relationship for the plateau phase (not shown) presumably due to residual tetramer internalization. Hence, the evaluation was confined to the initial 10 min that obeyed a linear relationship (Fig. 7*F* runs test) in analogy to Ref. 31); the half-lives of tetramer binding were $t_{1/2} = 11.4 \pm 0.7$ min for the Wt TCR MDM2 and $t_{1/2} = 9.6 \pm 0.8$ min for the matched TCR MDM2. The difference of their slopes was statistically not significant ($p = 0.2$). From this we conclude that the reciprocal mutations did not perturb Ag recognition.

Discussion

The main findings of this work are: 1) both Hu and Mu TCR chains can readily form hybrid TCR upon transduction into T lymphocytes, thus revealing a marked propensity to pair with unrelated TCR chains being synthesized in the same lymphocyte; and 2) we have identified by visual inspection of the 2C TCR crystal structure a pair of residues buried in the CαCβ interface that are critical for αβ pairing. These findings have important practical implications for future immunotherapy strategies based on gene transfer of high avidity TCR directed against viral or tumor Ags (1).

Cell surface expression reflects the intrinsic stability of a membrane protein such as the stabilization of HLA molecules that depends on peptide binding (39). As shown here, the expression of single TCR β-chains, irrespective of being of Mu or Hu origin, is conferred by the presence of their counterpart in a Mu hybridoma lacking endogenous TCR. Detection of a Mu TCR β-chain in Hu T cells is further increased by its humanization in Cβ and suggests a stabilizing effect by pairing to endogenous TCR α-chains. This reveals chain pairing as one of the major functions of TCR C-domains (40) and implies that heterologous expression of Hu or humanized TCR in Hu T cells causes the random combination of chains (11) leading to a plethora of hybrid TCR with unknown and potentially autoimmune specificities (9).

We further observed an inverse relationship between the level of Mu TCR MDM2 expression relative to endogenous Hu TCR expression. Correspondingly, murinization of a Hu TCR gp100 in $C\alpha\beta$ triggered down-regulation of endogenous TCR (Ref. 16 and data not shown). Thus, we assume that the Mu TCR α- and β-chains favorably associate to each other, provoking its thermal and/or proteolytic stabilization. This confers efficient competition with endogenous TCR for binding to the Hu CD3 complex, the shuttle for export to the cell membrane (16, 17). However, we cannot rule out a mechanism governed by a stretch of conserved residues in Mu C-domains to favor interaction to Hu CD3$\varepsilon\gamma$ (41).

Although different mechanisms of TCR/CD3 chain assembly prevail for introduced Hu and Mu TCR as outlined previously, the outcome of the reciprocal mutations for structural and functional avidity was the same: the complementarity matched TCR retain an efficiency comparable to that of Wt TCR while that of the unmatched TCR was highly reduced. This may be explained by, first, the importance of the chosen residues for the overall integrity of the TCR structure. Even intraspecies combinations of a Hu introduced and endogenous TCR C-domain, for which one may assume a high interchain affinity, were drastically affected by the replacement of either a small (Ser-85.1cα) or a bulky charged residue (Arg-88cβ). Second, we assume that, despite the favorable incorporation of Mu TCR chains into the Hu CD3-complex (16, 17), the assembly of Mu TCR chains resembles that of Hu TCR due to their high homology in primary and tertiary structure (18, 19). This is supported by our finding that the interchain affinity of a Mu and a Hu TCR is sufficiently high to form interspecies hybrid TCR.

The rational design of interfaces of Ig-like folded domains have been formerly studied in detail for Abs in P. Carter's laboratory. The reciprocal introduction of a pair of specifically interacting "knob-into-hole" residues Thr-366-Trp/Tyr'-407-Ala at the interface of the invariant C_H3 domains favored the generation of an anti-CD3/CD4-IgG heterodimer that has been further improved by "phage display" (32, 42). In this study we aimed at minimizing the impact on TCR structure by simply swapping the positions of native Gly-85.1cα or Ser-85.1cα and Arg-88cβ between the invariant Cα- and Cβ-domains, thus rendering both sterically (i.e., Van der Waals surface of side chains) and electrostatically (i.e., charge of arginine) unchanged except for their orientations.

The Cα-Cβ interface of the 2C TCR is characterized by high complementarity and polarity skewed by a predominant location of basic residues in Cβ and acidic and polar residues in Cα (18). The asymmetric charge distribution at the interface raises the question of the relative contributions of steric vs electrostatic interactions to chain pairing. In most experiments we observed a much more pronounced reduction in avidities for the Mtα/Wtβ combination than for the Wtα/Mtβ combination. Obviously, steric hindrance and electrostatic repulsion of two bulky and charged arginines facing each other is more detrimental to structural avidity than the lack of interaction and withdrawal of charge. From this we draw the conclusion that reciprocal mutations do not lead to preferential chain pairing in terms of an improved fitting but to prohibitive pairing to unmatched endogenous TCR. This shifts the heterodimerization equilibrium toward reciprocally designed TCR.

However, the poor recovery of single mutant TCRβ MDM2 in T cells is consistent with the idea that the withdrawal of charge also exerts a severe effect on chain pairing. The reduction of Van der Waals interactions by omission of the Arg-88cβ side chain should be compensated somewhat by the multitude of interactions along the vast buried CαCβ-surface area of ~2049 Å^2 (18). In light of the charge asymmetry in TCR C-domains (18), we propose that the charged guanidinium group of Arg-88cβ, as one of a few basic key amino acids (Fig. 1*B*), contributes to long-ranging electrostatic forces and a fast kinetic of C-domain association (33). Subsequently, the variable domains associate mainly governed by hydrophobic interactions (43) and may demand more time for proper assembly due to their TCR subfamily-related sequence degeneracy.

Hence, for the functional optimization of TCR chain pairing, the hypothesized two-step mechanism suggests that the last event should not be manipulated (i.e., chain pairing of the variable domains) because most of the decisive interactions, located in the C-domains, may have already formed at that time. This notion is consistent with the observations that the formation of heterodimeric constant domains of a truncated TCR is sufficient for stable surface expression (40) and that the large surface area of the CαCβ interface (2049 Å^2) overwhelms that of the variable domains (1160 Å^2; Ref. 18). These aspects account for the pivotal function of C-domains in heterodimerization. Moreover, the sequence degeneracy of the core V-domains (43), their hydrophobicity, and their close juxtaposition to the Ag recognition site complicates the identification of ideally suited (un)charged "knob-into-hole"- residues to apply to a subfamily-independent approach.

However, the tiny shift of the charged guanidinium group in mutated Arg-85.1cα toward the "basic" surface of Cβ may cause a structural alteration responsible for the slight decline in efficacy of the matched TCR. Currently, we are trying to optimize the reciprocal configuration by changing the size, charge, and potential hydrogen bonding of the involved residues. In an effort to endow each chain with a repulsive and charged knob, we introduced into the matched Mt Arg-85.1cα/Mt Gly-88cβ TCR vice versa an Ile-86cα-Gly/Ser-86cβ-Arg mutation in a juxtaposed position. Even the reduction of all bulky arginines to lysines in these 4-fold mutated heterodimers yielded nonfunctional TCR (data not shown). Hence, TCR structure turns out to be very susceptible to local alterations at its interface.

Recently, TCR have been stabilized by introducing an artificial disulfide bridge into the constant domain (14, 15). This approach may benefit from preferential pairing due to the formation of an irreversible covalent linkage but disregards the risk of hybrid TCR formation. Serine, threonine, and cysteine are chemically homologous and will hardly initiate steric repulsion or lack of interaction. This notion is supported by the fact that disulfide bridges are not necessary for TCR$\alpha\beta$ heterodimerization (40). As an objective, one may attempt to combine the advantageous effect of the reciprocal mutations with that of the artificial disulfide bridge.

Although the Wt TCR MDM2- and gp100-introduced T cells differed by a factor of 28 in cytotoxic efficiencies, the EC_{50} values revealed approximately a proportional reduction in peptide recognition for their unmatched TCR MDM2 (factor of 9–11) and TCR gp100 (factor of 7–46). Although they are still able to recognize titrated Ag in a low nanomolar range, recognition of tumor cell lines or transfectants was nearly abolished. Thus, the reciprocal mutation approach may be generalized to tumor-reactive TCR with a broad range of Ag affinities. Because the resulting avidity of T cells for their Ag equals the product of TCR cell surface density and its molecular affinity to the cognate peptide/MHC ligand, we conclude from first-order dissociation experiments that it is not a decreased TCR affinity but its diminished surface expression that causes the observed differences in structural and functional avidities between the Wt and matched TCR. Ag recognition needs a minimal avidity that, besides TCR affinity, also depends on heterodimerization for sufficient TCR expression (44).

In summary, we describe the successful rational design of TCR interfaces to promote specific chain pairing. This approach paves the way for the molecular refinement of TCR mutants that favorably interact by noncovalent modifications leaving the overall topology unchanged for optimal avidity and maximal reduction of potential immunogenicity.

Acknowledgments

We appreciate the contributions by Edite Antunes Ferreira for technical assistance, Martin Schuler for sharing reagents, and Abdo Konur and Magda Brkic for sorting T cells. In particular, we thank Hansjörg Schild for the critical review of this manuscript.

Disclosures

A patent is pending for Ralf-Holger Voss and Matthias Theobald.

References

1. Morgan, R. A., M. E. Dudley, J. R. Wunderlich, M. S. Hughes, J. C. Yang, R. M. Sherry, R. E. Royal, S. L. Topalian, U. S. Kammula, N. P. Restifo, et al. 2006. Cancer regression in patients after transfer of genetically engineered lymphocytes. *Science* 314: 126–129.
2. Theobald, M., J. Biggs, J. Hernandez, J. Lustgarten, C. Labadie, and L. A. Sherman. 1997. Tolerance to p53 by A2.1-restricted cytotoxic T lymphocytes. *J. Exp. Med.* 185: 833–841.
3. Stanislawski, T., R. H. Voss, C. Lotz, E. Sadovnikova, R. A. Willemsen, J. Kuball, T. Ruppert, R. L. Bolhuis, C. J. Melief, C. Huber, et al. 2001. Circumventing tolerance to a human MDM2-derived tumor antigen by TCR gene transfer. *Nat. Immunol.* 2: 962–970.
4. Kuball, J., F. W. Schmitz, R. H. Voss, E. A. Ferreira, R. Engel, P. Guillaume, S. Strand, P. Romero, C. Huber, L. A. Sherman, and M. Theobald. 2005. Cooperation of human tumor-reactive CD4$^+$ and CD8$^+$ T cells after redirection of their specificity by a high-affinity p53A2.1-specific TCR. *Immunity* 22: 117–129.
5. Li, Y., R. Moysey, P. E. Molloy, A. L. Vuidepot, T. Mahon, E. Baston, S. Dunn, N. Liddy, J. Jacob, B. K. Jakobsen, and J. M. Boulter. 2005. Directed evolution of human T-cell receptors with picomolar affinities by phage display. *Nat. Biotechnol.* 23: 349–354.
6. Holler, P. D., P. O. Holman, E. V. Shusta, S. O'Herrin, K. D. Wittrup, and D. M. Kranz. 2000. In vitro evolution of a T cell receptor with high affinity for peptide/MHC. *Proc. Natl. Acad. Sci. USA* 97: 5387–5392.
7. Kessels, H. W., M. D. van den Boom, H. Spits, E. Hooijberg, and T. N. Schumacher. 2000. Changing T cell specificity by retroviral T cell receptor display. *Proc. Natl. Acad. Sci. USA* 97: 14578–14583.
8. Kessels, H. W., M. C. Wolkers, M. D. van den Boom, M. A. van der Valk, and T. N. Schumacher. 2001. Immunotherapy through TCR gene transfer. *Nat. Immunol.* 2: 957–961.
9. Schumacher, T. N. 2002. T cell-receptor gene therapy. *Nat. Rev. Immunol.* 2: 512–519.
10. Naylor, K., G. Li, A. N. Vallejo, W. W. Lee, K. Koetz, E. Bryl, J. Witkowski, J. Fulbright, C. M. Weyand, and J. J. Goronzy. 2005. The influence of age on T cell generation and TCR diversity. *J. Immunol.* 174: 7446–7452.
11. Roszkowski, J. J., D. C. Yu, M. P. Rubinstein, M. D. McKee, D. J. Cole, and M. I. Nishimura. 2003. CD8-independent tumor cell recognition is a property of the T cell receptor and not the T cell. *J. Immunol.* 170: 2580–2589.
12. Zhang, T., X. He, T. C. Tsang, and D. T. Harris. 2004. Transgenic TCR expression: comparison of single chain with full length receptor constructs for T-cell function. *Cancer Gene Ther.* 11: 487–496.
13. Willemsen, R. A., M. B. Weijtens, C. Ronteltap, Z. Eshhar, J. W. Gratama, P. Chames, and R. L. Bolhuis. 2000. Grafting primary human T lymphocytes with cancer-specific chimeric single chain and two chain TCR. *Gene Ther.* 7: 1369–1377.
14. Kuball, J., M. L. Dossett, M. Wolfl, W. Y. Ho, R. H. Voss, C. Fowler, and P. D. Greenberg. 2007. Facilitating matched pairing and expression of TCR chains introduced into human T cells. *Blood* 109: 2331–2338.
15. Cohen, C. J., Y. F. Li, M. El-Gamil, P. F. Robbins, S. A. Rosenberg, and R. A. Morgan. 2007. Enhanced antitumor activity of T cells engineered to express T-cell receptors with a second disulfide bond. *Cancer Res.* 67: 3898–3903.
16. Voss, R. H., J. Kuball, R. Engel, P. Guillaume, P. Romero, C. Huber, and M. Theobald. 2006. Redirection of T cells by delivering a transgenic mouse-derived MDM2 tumor antigen-specific TCR and its humanized derivative is governed by the CD8 coreceptor and affects natural human TCR expression. *Immunol. Res.* 34: 67–87.
17. Cohen, C. J., Y. Zhao, Z. Zheng, S. A. Rosenberg, and R. A. Morgan. 2006. Enhanced antitumor activity of murine-human hybrid T-cell receptor (TCR) in human lymphocytes is associated with improved pairing and TCR/CD3 stability. *Cancer Res.* 66: 8878–8886.
18. Cecil, K. C., M. Pegiazo, R. L. Stanfield, A. Brunmark, M. R. Jackson, P. A. Peterson, L. Teyton, and I. A. Wilson. 1996. An $\alpha\beta$T cell receptor structure at 2.5 Å and its orientation in the TCR MHC complex. *Science* 274: 209–219.
19. Ding, Y. H., K. J. Smith, D. N. Garboczi, U. Utz, W. E. Biddison, and D. C. Wiley. 1998. Two human T cell receptors bind in a similar diagonal mode to the HLA-A2/Tax peptide complex using different TCR amino acids. *Immunity* 8: 403–411.
20. Lefranc, M. P. 2003. IMGT, the international ImMunoGeneTics database. *Nucleic Acids Res.* 31: 307–310.
21. Lefranc, M. P., C. Pommié, Q. Kaas, E. Duprat, N. Bosc, D. Guiraudou, C. Jean, M. Ruiz, I. Da Piédade, M. Rouard, et al. 2005. IMGT unique numbering for immunoglobulin and T cell receptor constant domains and Ig superfamily C-like domains. *Dev. Comp. Immunol.* 29: 185–203.
22. Schall, N., R. A. Willemsen, J. de Vries, B. Lankiewicz, B. W. Eisen, J. W. Gratama, C. G. Figdor, R. L. Bolhuis, R. Debets, and G. J. Adema. 2003. Peptide fine specificity of anti-glycoprotein 100 CTL is preserved following transfer of engineered TCR α β genes into primary human T lymphocytes. *J. Immunol.* 170: 2186–2194.
23. Bullock, T. N., D. W. Mullins, T. A. Colella, and V. H. Engelhard. 2001. Manipulation of avidity to improve effectiveness of adoptively transferred CD8$^+$ T cells for melanoma immunotherapy in human MHC class I-transgenic mice. *J. Immunol.* 167: 5824–5831.
24. Berman, H. M., J. Westbrook, Z. Feng, G. Gilliland, T. N. Bhat, H. Weissig, I. N. Shindyalov, and P. E. Bourne. 2000. The protein data bank. *Nucleic Acids Res.* 28: 235–242.
25. Guex, N., and M. C. Peitsch. 1997. Swiss-Model and the Swiss-PdbViewer: an environment for comparative protein modeling. *Electrophoresis* 18: 2714–2723.
26. Blank, U., B. Boitel, D. Mege, M. Ermonval, and O. Acuto. 1993. Analysis of tetanus toxin peptide/DR recognition by human T cell receptors reconstituted into a murine T cell hybridoma. *Eur. J. Immunol.* 23: 3057–3065.
27. Voss, R. H., J. Kuball, and M. Theobald. 2005. Designing TCR for cancer immunotherapy. *Methods Mol. Med.* 109: 229–256.
28. Grignani, F., T. Kinsella, A. Mencarelli, M. Valtieri, D. Riganelli, F. Grignani, L. Lanfrancone, C. Peschle, G. P. Nolan, and P. G. Pelicci. 1998. High-efficiency gene transfer and selection of human hematopoietic progenitor cells with a hybrid EBV/retroviral vector expressing the green fluorescence protein. *Cancer Res.* 58: 14–19.
29. Robert, B., P. Guillaume, I. Luescher, P. Romero, and J. P. Mach. 2000. Antibody-conjugated MHC class I tetramers can target tumor cells for specific lysis by T lymphocytes. *Eur. J. Immunol.* 30: 3165–3170.
30. Whelan, J. A., P. R. Dunbar, D. A. Price, M. A. Purbhoo, F. Lechner, G. S. Ogg, G. Griffiths, R. E. Phillips, V. Cerundolo, and A. K. Sewell. 1999. Specificity of CTL interactions with peptide-MHC class I tetrameric complexes is temperature dependent. *J. Immunol.* 163: 4342–4348.
31. Rosette, C., G. Werlen, M. A. Daniels, P. O. Holman, S. M. Alam, P. J. Travers, N. R. Gascoigne, E. Palmer, and S. C. Jameson. 2001. The impact of duration versus extent of TCR occupancy on T cell activation: a revision of the kinetic proofreading model. *Immunity* 15: 59–70.
32. Ridgway, J. B., L. G. Presta, and P. Carter. 1996. 'Knobs-into-holes' engineering of antibody CH3 domains for heavy chain heterodimerization. *Protein Eng.* 9: 617–621.
33. Schreiber, G., and A. R. Fersht. 1996. Rapid, electrostatically assisted association of proteins. *Nat. Struct. Biol.* 3: 427–431.
34. Clackson, T., and J. A. Wells. 1995. A hot spot of binding energy in a hormone-receptor interface. *Science* 267: 383–386.
35. Irving, B. A., and A. Weiss. 1991. The cytoplasmic domain of the T cell receptor ζ chain is sufficient to couple to receptor-associated signal transduction pathways. *Cell* 64: 891–901.
36. McKee, M. D., T. M. Clay, S. A. Rosenberg, and M. I. Nishimura. 1999. Quantitation of T-cell receptor frequencies by competitive PCR: generation and evaluation of novel TCR subfamily and clone specific competitors. *J. Immunother.* 22: 93–102.
37. Savage, P. A., and M. M. Davis. 2001. A kinetic window constricts the T cell receptor repertoire in the thymus. *Immunity* 14: 243–252.
38. Kersh, G. J., E. N. Kersh, D. H. Fremont, and P. M. Allen. 1998. High- and low-potency ligands with similar affinities for the TCR: the importance of kinetics in TCR signaling. *Immunity* 9: 817–826.
39. Holmberg, K., S. Marathuvan, I. Ohteki, P. S. Ohashi, and N. R. Gascoigne. 2003. TCR binding kinetics measured with MHC class I tetramers reveal a positive selecting peptide with relatively high affinity for TCR. *J. Immunol.* 171: 2427–2434.
40. Li, Z. G., W. P. Wu, and N. Manolios. 1996. Structural mutations in the constant region of the T-cell antigen receptor (TCR) β-chain and their effect on TCR α and β-chain interaction. *Immunology* 88: 524–530.
41. Sun, Z. Y., S. T. Kim, I. C. Kim, A. Fahmy, E. L. Reinherz, and G. Wagner. 2004. Solution structure of the CD3$\varepsilon\delta$ ectodomain and comparison with CD3$\varepsilon\gamma$ as a basis for modeling T cell receptor signaling. *Proc. Natl. Acad. Sci. USA* 101: 16867–16872.
42. Atwell, S., J. B. Ridgway, J. A. Wells, and P. Carter. 1997. Stable heterodimers from remodeling the domain interface of a homodimer using a phage display library. *J. Mol. Biol.* 270: 26–35.
43. Chothia, C., D. R. Boswell, and A. M. Lesk. 1988. The outline structure of the T cell $\alpha\beta$ receptor. *EMBO J.* 7: 3745–3755.
44. Labrecque, N., L. S. Whitfield, R. Obst, C. Waltzinger, C. Benoist, and D. Mathis. 2001. How much TCR does a T cell need? *Immunity* 15: 71–82.